International Scientific Organization
http://iscientific.org/
Chemistry International
www.bosaljournals.com/chemint/

Inhibition behavior of *Fadogia andersonii* Robyns leave extract for mild steel corrosion in acidic media: Electrochemical and surface investigation

Nkem B. Iroha*

Electrochemistry and Material Science Unit, Department of Chemistry, Federal University Otuoke, Nigeria
*Corresponding author's E. mail: irohanb@fuotuoke.edu.ng

ARTICLE INFO	ABSTRACT
	The aim of this research is to evaluate the effectiveness *Fadogia andersonii* Robyns (FAR) as a corrosion inhibitor for mild steel in an acidic media (1 *M* HCl). The corrosion inhibition of FAR was characterized by surface morphology, potentiodynamic polarization, electrochemical impedance spectroscopy (EIS) and weight loss methods. The results showed that inhibitor performance depends on both concentration and temperature. The inhibition efficiency decreases with increasing the temperature from 303 to 323 K but increases with increase in concentration, reaching a maximum value of 91.0% at the highest concentration of 300 ppm at the temperature of 303 K; from weight loss measurement. Polarization study revealed that the extract behaves as mixed-type inhibitor. The inhibitor molecules adsorb on the surface of the metal, following Langmuir`s adsorption isotherm The micrograph from SEM showed that the inhibitor adsorbed onto the metal surface which indicate less damage on the metal surface in the presence of FAR.

Capsule Summary: *Fadogia andersonii* Robyns extract as a corrosion inhibitor for mild steel in 1 M HCl solution was investigated and the extract showed promising efficiency for corrosion inhibition at optimum conditions of process variable.

INTRODUCTION

Corrosion is the one of the biggest problems in industries which leads to increase of maintenance expenditure, product contamination, economic loss, structural failure etc. Mild steel has been used under different conditions in chemical and allied industries. Most times, mild steel is exposed to the attack of acid solutions during industrial processes such as acid cleaning, pickling and descaling. The most common method for corrosion control is the use of corrosion inhibitors (Yıldız et al., 2014; Iroha et al., 2021). A corrosion inhibitor is a chemical compound or combination of compounds that, when introducing in the appropriate concentration and forms in the environment, reduces corrosion (Bensouda et al., 2018). The general corrosion rate may be extremely high and increase exponentially with increasing temperature and acid concentrations, in the absence of corrosion inhibitors (Kumar and Yadav, 2013). Natural plant extracts are effective green corrosion inhibitors for mild steel and were found to be cheaper, more efficient, renewable, biodegradable and environmentally friendly method of inhibiting corrosion rate in mild steel (Chigondo and Chigondo, 2016; Kavitha et al., 2014; Njoku and Onyelucheya, 2015: James and Iroha, 2021). The environmental friendliness of plants extracts has extended its

application frontiers even to the oil and gas industries and hence its popularity and acceptability, making corrosion inhibition studies on the use of plants extracts a very active field.

Fadogia andersonii Robyns (FAR) is an erect undershrub of about 1-2 ft. high, stems more or less 3-angled from a stout woody rootstock, branchlets glabrous; leaves paired or in threes, oblanceolate. Flowers are greenish-yellow while fruit yellow (Hutchison and Dalziel, 1963). The plant is called by different Hausa speakers as Bita Katsira, Dan Goyo or Gagai depend on the uses. It is native to Burkina, Benin, Nigeria, Togo and Ghana. The plant is a popular African medicinal plant, which has long been used in Africa in treatment of diseases including amoebic dysentery, dried powdered leaf in hot infusion for the cure of inflammation, malaria, arthritis, fractures, colicky pain and typhoid. Powdered leaf mix with oil to cure wounds and boils. The aqueous roots extract increases sperm count, epididymal weight and motility (Suleiman et al., 2014).

The leave extract of FAR contain cutin, cellulose, lignin, starch, tannins and gum & mucilage (Imam et al., 2022), indicating that these biologically active compounds are good adsorbents on the metal surface. This present study reports the inhibition behavior of FAR as a cheap, eco-friendly and naturally occurring substance on mild steel sheets in 1 M HCl solution by employing weight loss and electrochemical techniques (EIS and PDP). Surface analyses were performed on the corroded surfaced using scanning electronic microscopy (SEM).

MATERIAL AND METHODS

Solutions and sample preparation

The aerial part of FAR plant was procured from the Herbarium unit, Department of Botany, University of Port Harcourt. The leaves of the plant collected were washed and then air dried under shade at room temperature, ground to powder and stored in an air tight container for further use. A 25g of powder was macerated in 100ml of distilled water under magnetic agitation for 2 hours at 30 °C. After filtration, the aqueous extract was evaporated in an incubator for 2 to 3 days at 40 °C and stored as the stock solution of the inhibitor. The aggressive solutions of 1 M HCl were prepared by dilution of an analytical grade 37% HCl with double distilled water. The inhibitor concentrations; 100, 200 and 300 ppm were prepared from the stock solution.

Mild steel specimens of size 2 cm ×1 cm × 0.02 cm (weight % composition: C - 0.0691, Mn - 0.0389, S - 0.0009, P - 0.0221, Cr - 0.0463, Mo - 0.0667, Al - 0.0154, V - 0.03347 and remainder Fe) were utilized in weight loss experiments and also for electrochemical measurements. The mild steel coupons for electrochemical measurement were embedded in a Teflon holder using epoxy resin, exposing a surface area of 1 cm^2. The coupons were mechanically polished using emery paper of grades no. 800, 1000 and 1200, thoroughly washed with deionized water, and finally degreased with acetone prior to each measurement.

Electrochemical measurements

The electrochemical measurements were conducted in a conventional three electrodes glass cell using CHI 660C electrochemical analyzer. Mild steel, platinum foil and saturated calomel electrode (SCE) were used as working, counter and reference electrodes respectively. The temperature of the electrolyte was maintained at room temperature (30 ◦ C). The mild steel specimen was exposed to a corrosive medium of 1 M HCl in the presence or the absence of FAR at different temperatures and allowed to establish a steady state open circuit potential (OCP). The EIS experiments were conducted in the frequency range with high limit of 100 kHz and different low limit 0.1 Hz at open circuit potential, with 10 points per decade, at the rest potential, after 30 min of acid immersion, by applying 10 mV ac voltage peak-to-peak. Potentiodynamic polarization measurements were carried out at a scan rate of 1 mV/s by polarizing the specimen from −250 mV cathodically to +250 mV anodically, with respect to the OCP, and the PDP plots were recorded. To ensure the reproducibility of the measurements, each test was repeated three times and the average values were reported.

Weight loss measurement

The weight loss experiments were carried out in a glass vessel containing 100 mL of 1 M HCl with and without the addition of different concentrations (100 - 300 ppm) of FAR for about 6 h immersion time at 30, 40 and 50 °C. The temperature was controlled by an aqueous thermostat bath. Mild steel coupons were weighed after and before immersion time to record the weight loss. By the help of weight losses, corrosion rate and inhibition efficiency were calculated. To test reliability and reproducibility of the measurements, triplicate experiments were performed in each case of the same conditions.

Surface analysis

For the purpose of surface analysis, mild steel specimens with freshly pretreated surface as described in Section 2.1 were utilized. The scanning electron microscopy (FEG SEM, SUPRA 40VP, ZEISS, Germany) was used to study the morphology of the mild steel surface. The cleaned mild steel specimens were allowed to corrode for 6 h in absence and presence of optimum concentration of FAR. Thereafter, the specimens were taken out washed with water, dried and employed for SEM.

RESULTS AND DISCUSSION

Polarization curves
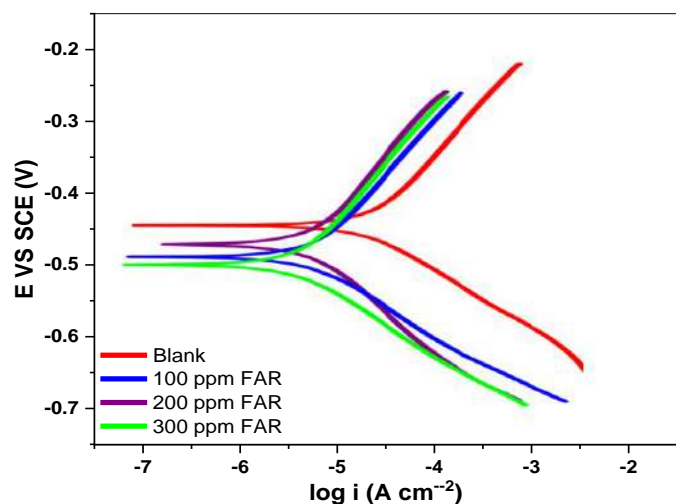
Fig. 1: Potentiodynamic polarization curves of mild steel in 1 M HCl solutions in the absence and presence of various concentrations of FAR at 30 °C.
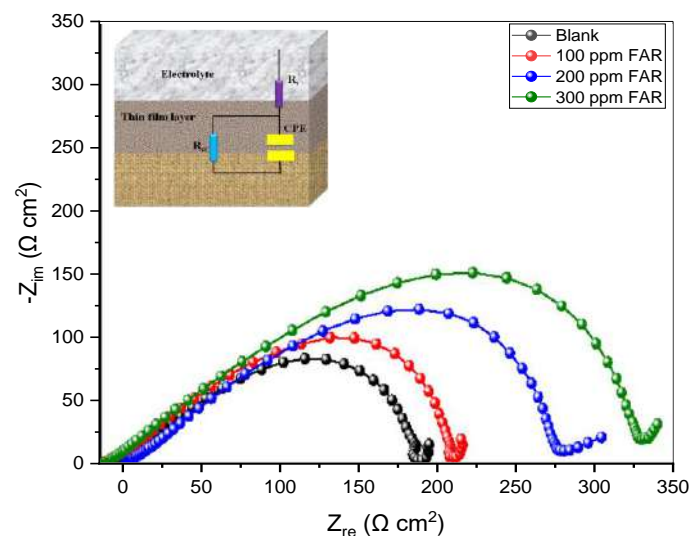
Fig. 2: The Nyquist plots for mild steel electrode in 1 M HCl without and with various concentrations of FAR at 30 °C (insert: equivalent circuit).

Figure 1 presents the potentiodynamic polarization curves of mild steel in 1 M HCl without and with the studied FAR inhibitor at 100 - 300 ppm and 30, 40 and 50 °C. The curves are shifted to lower current regions in the presence of inhibitor showing that the studied FAR inhibit the corrosion reaction. Kinetic parameters such as the corrosion potential (E_{corr}), corrosion current density (i_{corr}), anodic and cathodic Tafel slopes (βa and βc respectively) were obtained and reported in Table 1. The inhibition efficiency (*%IE$_{PDP}$*) was evaluated from the measured i_{corr} values using Eq. 1.

$$\%IE_{PDP} = \frac{i^0_{corr} - i_{corr}}{i^0_{corr}} \times 100 \qquad (1)$$

Where i^0_{corr} and i_{corr} are the corrosion current densities in the absence and presence of the FAR, respectively. The results in Table 1 showed the decrease in i_{corr} in presence of inhibitor as compared to blank solution in absence and presence of inhibitor. This is due to adsorption of inhibitor on metal surface which penetrates rate of corrosion current density and increases inhibition efficiency (Singh et al., 2013; Iroha and James, 2019). Table 1 also indicates that the values of βa and βc change significantly in the presence of FAR, therefore inhibitory molecules can be adsorbed to anodic and cathodic sites. A compound can only be regarded as either a anodic or cathodic inhibitor when the change in the E_{corr} value between the inhibited and the blank system is greater than 85 mV (Maduelosi and Iroha, 2020; Caldona et al., 2020). Therefore, FAR could be classified as a mixed type inhibitor, but under prominent cathodic control.

Electrochemical impedance spectroscopy

EIS technique was also used to assess the performance of FAR in 1 M HCl solution. EIS measures electrochemical changes *in situ*, which enables the physical processes occurring at the metal/electrolyte interface to be monitored (Verma et al., 2015; Abdel Nazeer et al., 2013). Nyquist plots in absence and presence of different concentrations of inhibitor at 303 K are shown in Fig. 2. It is obvious that the EIS spectra of the inhibitor's free solution and the EIS spectra of the inhibitor containing solutions show similar characteristics suggesting that mechanism of mild steel corrosion is similar in both the cases. A depressed semicircle, representing the roughness of the tested sample's surface, can be seen in all Nyquist diagrams, indicating that the corrosion of mild steel is mainly controlled by charge transfer process at electrode/solution interface (Iroha et al., 2023; Valcarce et al., 2009; Iroha et al., 2022; Singh et al., 2022). After addition of inhibitors, the diameter of the capacitive loops increased with increase in the inhibitor concentration suggesting that FAR act as efficient corrosion inhibitors for mild steel. Insert in Fig. 2 represents an equivalent circuit used in the present study to analyze the electrochemical impedance data. The equivalent circuit consists of solution resistance (R_s), charge transfer resistance (R_{ct}), a constant phase element (*CPE*); a CPE has been used in place of double layer capacitance (C_{dl}) in order to accurately fit the circuit. The impedance of the CPE (Z_{CPE}) can be represented by the expression shown in Eq. 2.

$$Z_{CPE} = \frac{1}{Q}(j\omega)^{-n} \qquad (2)$$
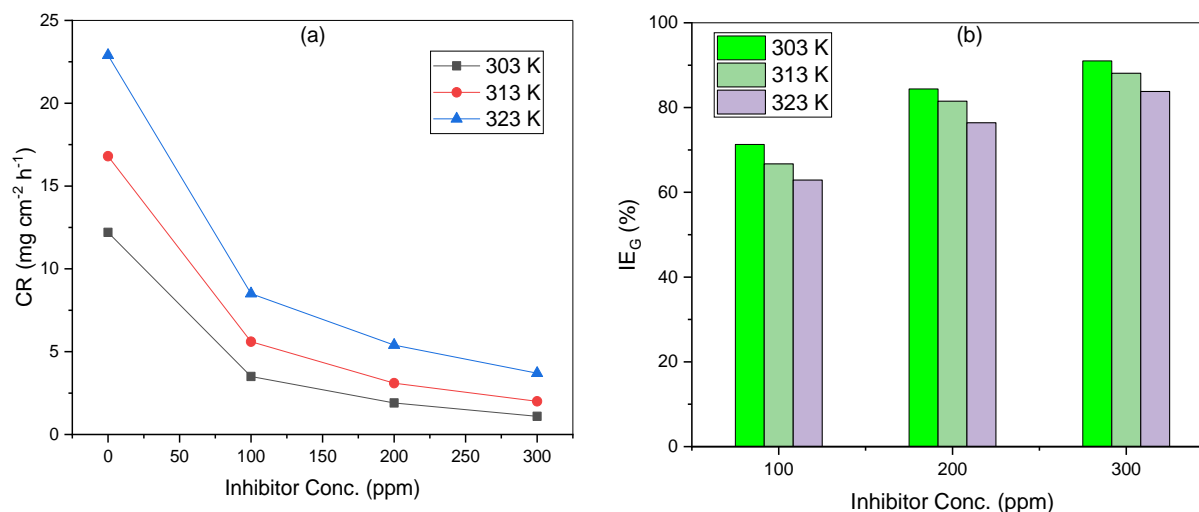
Fig. 3: Variation in corrosion rate and inhibition efficiency at different concentrations of FAR by weight loss
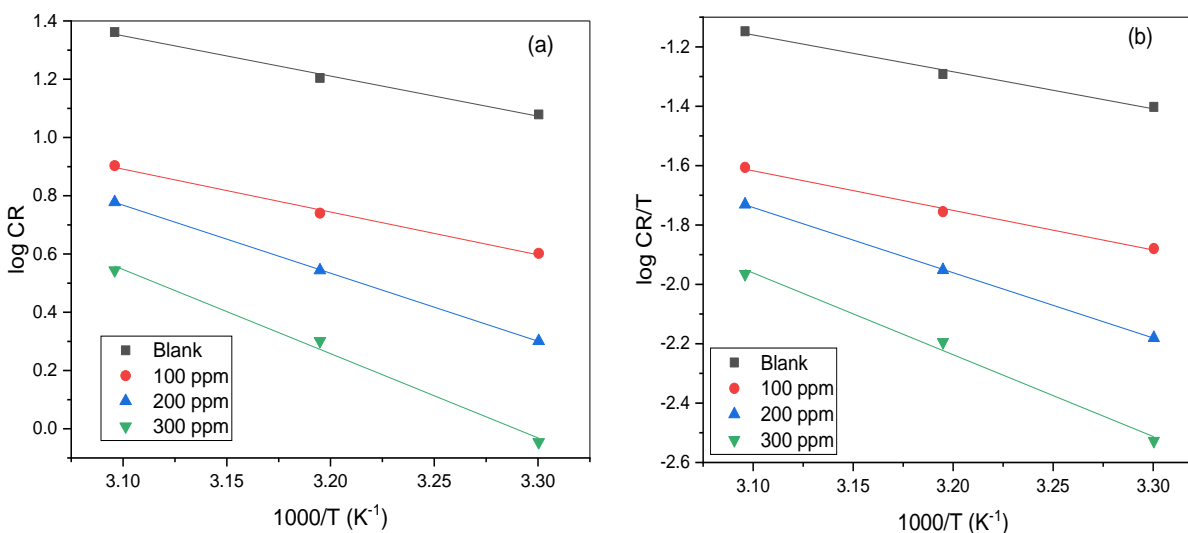
Fig. 4: (a) Arrhenius plots of log CR vs 1/T and (b) Transition-state plots of log (CR/T) vs 1/T for mild steel in 1 M HCl with and without different concentrations of FAR

Where, Q is the proportionality constant and comparable to capacitance, j is the imaginary unit and ω is the angular frequency ($\omega = 2\pi f_{max}$; f_{max} is the frequency at maximum in Hz), and n is phase shift and related to degree of surface non-homogeneity. The C_{dl} values are calculated using Eq. 3 (Pandey et al., 2017; Aslam et al., 2017; Iroha and Nnanna, 2021).

$$C_{dl} = Q(\omega_{max})^{n-1} \qquad (3)$$

Where, ω_{max} is the angular frequency at which the imaginary part of the impedance is maximum. The inhibition efficiency ($\%IE_{EIS}$) is calculated from the charge transfer resistance (R_{ct}) as shown in Fig. 4.

$$\%IE_{EIS} = \frac{R_{ct(inh)} - R_{ct}}{R_{ct(inh)}} \times 100 \qquad (4)$$

Where, R_{ct} and $R_{ct(inh)}$ are the values of charge transfer resistance in the absence and the presence of inhibitor in 1 M HCl, respectively. The EIS parameters are given in Table 2. The data show that the R_{ct} values increases and the C_{dl} values decreases with increasing the inhibitor concentrations. This is due to the formation of protective film on the surface of mild steel by the addition of various concentrations of inhibitor, resulting in an increase in the inhibition efficiency. The high values of R_{ct} are generally associated with slower corroding system. The decrease in the C_{dl} can result from the decrease of the local dielectric constant and/or from the increase of thickness of the electrical double layer suggested that the inhibitor molecules function by adsorption at the metal/solution interface. The inhibition efficiency obtained from EIS measurements are in agreement with those deduced from polarization measurements.

89
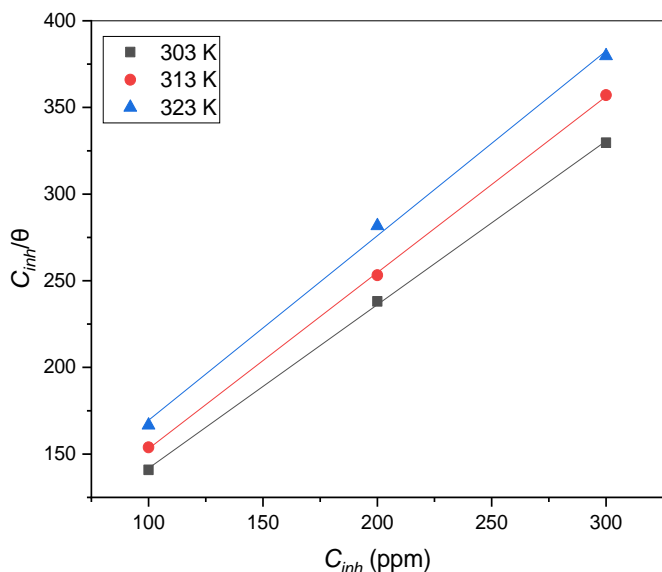
Fig. 5: Langmuir adsorption isotherm plot for FAR in 1 M HCl for the corrosion of mild steel

Gravimetric studies

Figure 3(a-b) shows corrosion rate (CR) and inhibition efficiency ($\%IE_G$) of mild steel in 1 M HCl with different concentrations of FAR at 303, 313 and 323 K, respectively. The CR and $\%IE_G$ values can be calculated by using relation shown in Eq. 5 and 6, respectively.

$$CR = \frac{\Delta W}{At} \tag{5}$$

$$\%IE_G = \frac{C_{R(blank)} - C_{R(inh)}}{C_{R(blank)}} \times 100 \tag{6}$$

Where, A (cm^2) is the exposed area of the steel samples, t is the exposure time of the mild steel specimens, $C_{R(blank)}$ and $C_{R(inh)}$ are the corrosion rates of mild steel in blank and inhibited solution, respectively. It can be seen from Fig.3a the CR value of mild steel observably decreased as the inhibitors were added. However, the inhibition efficiency increases with increasing concentration of the inhibitor and maximum value of inhibition efficiency of 91.0% was obtained at 300 ppm concentration and 303 K. The results indicated that the presence of FAR could effectively inhibit the corrosion of mild steel in 1 M HCl, and the high inhibition efficiency of FAR could be attributed to the adsorption of the inhibitor on the steel surface (Iroha et al. 2005).

Effect of temperature

Temperature has a great effect on the rate of metal electrochemical corrosion. The influence of temperature was studied by performing the weight loss experiments in the absence and presence of different concentrations of the FAR for 6 h immersion time in the temperature range of 303-323 K. As seen from Fig. 3, it is evident that the values of CR increased with the temperature in both uninhibited and inhibited solutions, which can be attributed to the desorption of initially adsorbed inhibitor molecules, leading to the exposure of a large metal surface area to corrosive media; therefore, the efficiency of the inhibitor decreases at higher temperatures. This implies that FAR is a temperature-related corrosion inhibitor.

The apparent activation energies (E_a) for mild steel corrosion in 1 M HCl solution in the presence and absence of FAR were evaluated from Arrhenius relation as shown in Eq. 7.

$$\log CR = \frac{-E_a}{2.303RT} + \log A \tag{7}$$

Where, A is the pre-exponential factor, R is the universal gas constant and T is the absolute temperature. Plotting log CR versus 1/T gives a straight line, as revealed by Fig. 4a.
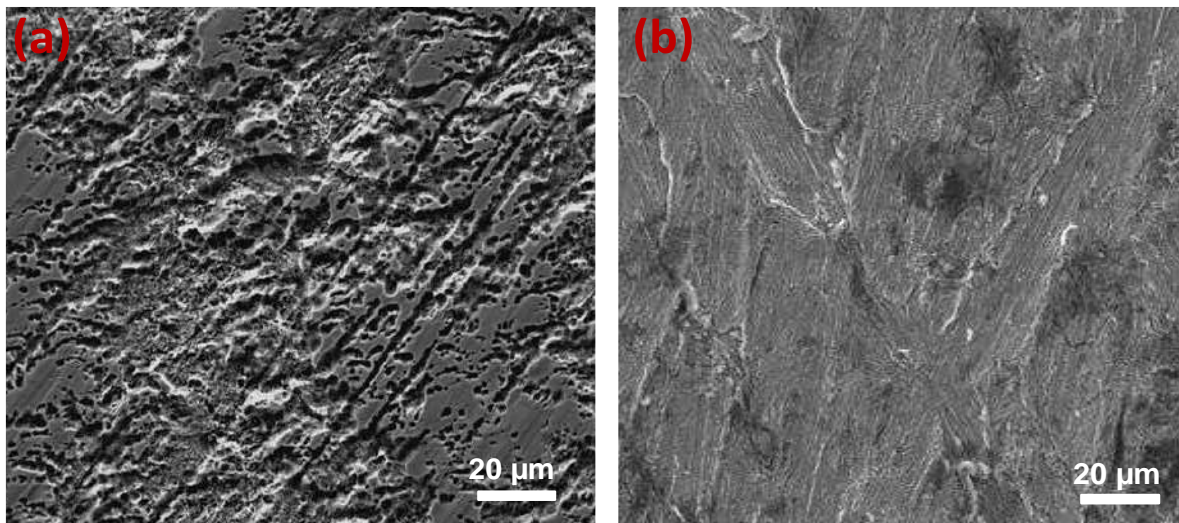
Fig. 6: SEM pictures of (a) mild steel in 1 M HCl, (b) mild steel in 300 ppm FAR

Table 1: Polarization data for mild steel in 1 M HCl in the absence and presence of various concentrations of FAR

Conc. (ppm)	E_{corr} (mV/SCE)	i_{corr} (µA cm^{-2})	β_a (mV dec^{-1})	$-\beta_c$ (mV dec^{-1})	IE PDP (%)
Blank	-447.8	690.2	215.7	194.1	-
100	-488.3	235.4	124.1	116.5	65.9
200	-473.6	118.7	103.5	97.4	82.8
300	-501.2	54.9	86.9	75.2	92.0

Table 2: EIS parameters of mild steel in 1 M HCl with and without FAR in various concentrations at 30 °C

Conc. (ppm)	R_s (Ω cm^2)	R_{ct} (Ω cm^2)	C_{dl} (µF cm^{-2})	n	IE_{EIS} (%)
Blank	1.26	21.4	199.0	0.893	-
100	1.08	58.1	124.1	0.916	63.2
200	1.47	126.9	83.7	0.943	83.1
300	1.55	245.1	16.3	0.952	91.3

Table 3. Activation energy (E_a), activation enthalpy (ΔH*) and activation entropy (ΔS*) for mild steel in 1 M HCl without and with various concentrations of FAR

Conc. (ppm)	E_a (kJ/mol)	ΔH^* (kJ/mol)	ΔS^* (J/mol/K)
Blank	31.62	27.32	-145.68
100	36.80	30.48	-131.73
200	39.31	33.53	-127.96
300	43.11	35.97	-123.61

Table 4: Adsorption parameters for corrosion inhibition of FAR on mild steel in 1 M HCl at different temperatures

Temp. (K)	Intercept	Slope	R^2	K_{ads} (ppm^{-1})	ΔG^0_{ads} (kJ/mol)
303	47.38	0.9441	0.9997	0.021	-28.53
313	51.42	1.0165	0.9998	0.019	-30.62
323	62.95	1.0654	0.9979	0.016	-31.99

The values of activation energy E_a obtained from the slope of the lines are given in Table 3. Inspection of Table 3 reveals that the values of E_a in presence of various concentrations of FAR were higher than that in absence of the inhibitor, indicating physical adsorption (Larabi et al., 2007). The enthalpy and entropy of activation (ΔH* and ΔS*, respectively) of the process can be obtained by the transition state equation (Eq. 8), as listed in Table 3.

$$\log \frac{C_R}{T} = \log \left(\frac{R}{Nh} \right) + \left(\frac{\Delta S^*}{2.303R} \right) - \left(\frac{\Delta H^*}{2.303RT} \right) \qquad (8)$$

Where, h is Planck's constant, N is the Avogadro number, and R is the universal gas constant, the plot of log (CR/N) versus $1/N$ (Fig. 4b) gives straight lines with a slope equal to −(ΔH*/2.303R) and an intercept (log(N/Nh) + (ΔS*/2.303R)) from which ΔH* and ΔS* values were calculated and listed in Table 3. The positive sign of enthalpies reflects the endothermic nature of the steel dissolution process inferring that the dissolution of mild

steel is difficult. The negative values of ΔS* might be explained in the following way: before the adsorption of the inhibitor onto the metal surface, inhibitor molecules might freely move in the bulk solution, but with the progress in the adsorption, inhibitor molecules were orderly adsorbed onto the metal surface, and as a result, there was a decrease in entropy (Karthik and Sundaravadivelu, 2013).

Adsorption isotherm

Adsorption isotherms explain the degree of interaction of molecules of various inhibitors with the metal surface (Ashish and Quraishi, 2010). To understand the adsorption behavior of FAR on mild steel surface, the experimental data were tested on several adsorption isotherms. It is found that adsorption of FAR on mild steel surface in HCl solution follows the Langmuir adsorption isotherm for which a relation is shown in Eq. 9 (Machnikova et al., 2008; Iroha et al., 2012).

$$\frac{C_{inh}}{\theta} = \frac{1}{K_{ads}} + C_{inh} \tag{9}$$

Where, K_{ads} is the equilibrium constant for the metal-inhibitor interaction, C_{inh} is the inhibitor concentration and θ is the surface coverage. The plot of C_{inh}/θ vs C_{inh} in Fig. 5 is seen to be linear with regression coefficient (R^2) and slope close to 1, suggesting that the experimental data follow the Langmuir isotherm. The slight deviations of the slopes of the Langmuir plots from unity are due to the interactions between the adsorbed molecules on the metal surface as well as change in the heat of adsorption with increasing surface coverage (Bouyanzer et al., 2006). K_{ads} values, which indicate the binding power of the inhibitor to the steel surface, can be calculated from the intercept ($1/K_{ads}$) of the straight lines on the C_{inh}/θ axis. Furthermore, the standard free energy change (ΔG_{ads}^0) values for the adsorption were calculated using Eq. 10.

$$K_{ads} = \frac{1}{55.5} \exp\left(\frac{-\Delta G_{ads}^0}{RT}\right) \tag{10}$$

Where, R is the gas constant (8.314 J·K^{-1}·mol^{-1}), 55.5 is the molar concentration (mol·L^{-1}) of water in the solution and T is the absolute temperature in Kelvin. The calculated values of K_{ads} and ΔG_{ads}^0 are given in Table 4. The values of ΔG_{ads}^0 are negative indicating that the adsorption process proceeds spontaneously and the adsorbed layer on the mild steel surface is stable (Popova et al., 2003). Generally, the values of ΔG_{ads}^0 up to -20 kJ mol^{-1} are consistent with the electrostatic interaction between the charged molecules and the charged metal (physical adsorption) while those more negative than -40 kJ mol^{-1} involve sharing or transfer of electrons from the inhibitor molecules to the metal surface to form a coordinate type of bond (chemisorption) (Aljourani et al., 2009; Iroha and Dueke-Eze, 2021). As seen from Tables 4, the values of ΔG_{ads}^0 decrease as temperature increases and within the range; -28.53 to -31.99 kJ mol-1, suggesting chemical and physical adsorption for inhibitor in 1 M HCl.

Surface morphology

The mild steel surface was analyzed by SEM after immersion in 1.0 M HCl with and without 300 ppm FAR for 6 h at 30 °C, as shown in Fig. 6. The SEM image of mild steel coupon before immersion in the 1 M HCl solution containing no inhibitor (Fig. 6a), revealed the presence of porous layers full of micro cracks. Compared with the unprotected one, the inhibited surface had a lower permeability for aggressive particles. Consequently, the mild steel surface was effectively protected by FAR, validating the gravimetric and electrochemical results.

CONCLUSION

The current study sought to explore the application of FAR extract as an effective corrosion inhibitor for mild steel in 1

M HCl. The greater the inhibitor concentration, the better is the corrosion inhibition effect. The electrochemical test results show that FAR can inhibit the cathodic and anodic reactions in the corrosion process and belong to a mixed-type corrosion inhibitor. The weight loss study revealed that 91% inhibition efficiency was observed in controlling corrosion of mild steel in the acid solution containing optimum concentration of FAR (300 ppm) at 303 K. Surface coverage and inhibition efficiency data analyses revealed that the inhibitor was adsorbed on the metal surface, following the Langmuir adsorption isotherm. SEM study confirmed that a protective film was formed on the metal surface.

REFERENCES

Abdel Nazeer, A., El-Abbasy, H., Fouda, A., 2013. Antibacterial drugs as environmentally-friendly corrosion inhibitors for carbon steel in acid medium. Research on Chemical Intermediates 39, 921-939.

Aljourani, J., Raeissi, K., Golozar, M.A., 2009. Benzimidazole and its derivatives as corrosion inhibitors for mild steel in 1 M HCl solution. Corrosion Science 51, 1836-1843.

Aslam, R., Mobin, M., Aslam, J., Lgaz, H., 2018. Sugar based N, N′-didodecyl-N, N′ digluconamideethylenediamine gemini surfactant as corrosion inhibitor for mild steel in 3.5% NaCl solution-effect of synergistic KI additive. Scientific Reports 8, Article number: 3690.

Bensouda, Z., Elassiri, E., Galai, M., Sfaira, M., Farah, A., Ebn Touhami, M., 2018. Corrosion inhibition of mildsteel in 1 M HCl solution by *Artemisia Abrotanum* essential oil as an eco-friendly inhibitor. Journal of Materials and Environmental Sciences 9(6), 1851-1865.

Bouyanzer, A., Hammouti, B., Majidi, L., 2006. Pennyroyal oil from Mentha pulegium as corrosion inhibitor for steel in 1 M HCl. Materials Letters 60, 2840–2843.

Caldona, E.B., Zhang, M., Liang, G., Hollis, T.K., Webster, C.E., Smith Jr, D.W., Wipf, D.O., 2020. Corrosion inhibition of mild steel in acidic medium by simple azole-based aromatic compounds. Journal of Electroanalytical Chemistry 880, 114858.

Chigondo, M., Chigondo, F., 2016. Recent natural corrosion inhibitors for mild steel: an overview. Journal of Chemistry Article ID 6208937.

Hutchison, J., Dalziel, J.M. 1963. Flora of west Tropical Africa (2nd ed./edited by Hepper, F.N. Vol. 2, pp.177-178). London, Millbank: crown agents for overseas Governments & Administrations.

Imam, K.I., Ahmed, A., Ambi, A.A, 2022. Pharmacognostic and physicochemical analysis of the leaves of Fadogia andersonii Robyns (Rubiaceae).

Iroha, N.B., Akaranta, O., James, A.O., 2012. Corrosion Inhibition of Mild Steel in Acid Media by Red Peanut skin extract-furfural Resin. Advances in Applied Science Research, 3(6), 3593-3598.

Iroha, N.B., Anadebe, V.C., Maduelosi, N.J., Nnanna, L.A., Isaiah, L.C., Dagdag, O., Berisha, A., Ebenso, E,E., 2023. Linagliptin drug molecule as corrosion inhibitor for mild

steel in 1 M HCl solution: Electrochemical, SEM/XPS, DFT and MC/MD simulation approach. Colloids and Surfaces A: Physicochemical and Engineering Aspects 660, 130885.

Iroha, N.B., Dueke-Eze, C.U. 2021. Experimental Studies on Two Isonicotinohydrazide-Based Schiff Bases as New and Efficient Inhibitors for Pipeline Steel Erosion Corrosion in Acidic Cleaning Solution. Chemistry Africa 4, 635–646.

Iroha, N.B., Dueke-Eze, C.U., James, A.O., Fasina, T.M., 2021. Newly synthesized N-(5-nitro-2-hydroxybenzylidene) pyridine-4-amine as a high-potential inhibitor for pipeline steel corrosion in hydrochloric acid medium. Egyptian Journal of Petroleum, 30, 55–61.

Iroha, N.B., James, A.O., 2019. Adsorption behavior of pharmaceutically active dexketoprofen as sustainable corrosion Inhibitor for API X80 carbon steel in acidic medium. World News of Natural Sciences, 27, 22-37.

Iroha, N.B., Nnanna, L.A., 2021. Tranexamic Acid as Novel Corrosion Inhibitor for X60 Steel in Oil Well Acidizing Fluids: Surface Morphology, Gravimetric and Electrochemical Studies. Progress in Color, Colorants and Coatings 14:1-11.

Iroha, N.B., Nnanna, L.A., Maduelosi, N.J., Anadebe, V.C., Abeng, F.E., 2022. Evaluation of the anticorrosion performance of Tamsulosin as corrosion inhibitor for pipeline steel in acidic environment: experimental and theoretical study. Journal of Taibah University for Science 16(1):288–299.

Iroha, N.B., Oguzie, E.E., Onuoha, G.N, Onuchukwu, A.I., 2005. Inhibition of Mild Steel Corrosion in Acidic Solution by derivatives of Diphenyl Glyoxal. 16th International Corrosion Congress, Beijing, China, 26-131

James, A.O., Iroha, N.B., 2021. New green inhibitor of Olax subscorpioidea root for J55 carbon steel corrosion in 15% HCl: theoretical, electrochemical, and surface morphological investigation. Emergent Mater 5, 1119–1131.

Karthik, G., Sundaravadivelu, M., 2013. Inhibition of Mild Steel Corrosion in Sulphuric Acid Using Esomeprazole and the Effect of Iodide Ion Addition. ISRN Electrochemistry Article ID 403542.

Kavitha, N., Manjula, P., Anandha, N., 2014. Syneristic effect of C. papaya leaves extract-Zn^{2+} in corrosion inhibition of mild steel in aqueous medium. Research Journal of Chemical Sciences 8, 88–93.

Kumar, H., Yadav, V., 2013. Corrosion characteristics of mild steel under different atmospheric conditions by vapour phase corrosion inhibitors. American Journal of Materials Science and Engineering 1, 34 -39.

Larabi, L., Benali, O., Harek, Y., 2007. Corrosion inhibition of cold rolled steel in 1 M HClO4 solutions by N-naphtyl N′-phenylthiourea. Materials Letters 61, 3287 - 3291.

Machnikova, E., Whitmire, K.H., Hackerman, N. 2008. Corrosion inhibition of carbon steel in hydrochloric acid by furan derivatives. Electrochimica Acta 53, 6024-6032.

Maduelosi, N.J., Iroha, N.B., 2020. Insight into the Adsorption and Inhibitive Effect of Spironolactone Drug on C38 Carbon Steel Corrosion in Hydrochloric Acid Environment. Journal of Bio- and Tribo-Corrosion 7, Article number: 6.

Njoku, C.N., Onyelucheya, O.E., 2015. Response surface optimization of the inhibition efficiency of Gongronema latifolium as an inhibitor for aluminium corrosion in HCl Solutions. International Journal of Materials and Chemistry 1, 4–13.

Pandey, A., Singh, B., Verma, C., Ebenso, E.E., 2017. Synthesis, characterization and corrosion inhibition potential of two novel Schiff bases on mild steel in acidic medium. RSC Advances. 7(74), 47148–47163.

Popova, A., Sokolova, E., Raicheva, S., Chritov, M., 2003. AC and DC study of the temperature effect on mild steel corrosion in acid media in the presence of benzimidazole derivatives. Corrosion Science 45, 33-58.

Singh, A., Ansari, K.R., Alanazi, A.K., Quraishi, M.A., Banerjee, P., 2022. Biological macromolecule as an eco-friendly high temperature corrosion inhibitor for P110 steel under sweet environment in NACE brine ID196: Experimental and computational approaches. Journal of Molecular Liquids. 345, 117866.

Singh, A., Ahamad, I., Quraishi, M.A., 2013. Piper longum extract as green corrosion inhibitor for aluminium in NaOH solution. Arabian Journal of Chemistry 9(2), S1584-S1589.

Suleiman, I., Mabrouk, A.M., Alhassan, W.A., 2014. Effect of aqueous root extract of Fadogia andersonii on sperm count and motility in adult male Wistar rats. Annals of Biological Sciences, 2 (4), 33-36.

Valcarce, M.B., Vàzquez, M., 2009. Carbon steel passivity examined in solutions with a low degree of carbonation: the effect of chloride and nitrite ions. Materials Chemistry and Physics 115 (1), 313–321.

Verma, C.B., Quraishi M. A., Singh, A., 2015. 2-Aminobenzene-1,3-dicarbonitriles as green corrosion inhibitor for mild steel in 1M HCl: Electrochemical, thermodynamic, surface and quantum chemical investigation. Journal of the Taiwan Institute of Chemical Engineers 49, 229–239.

Yıldız, R., Döner, A., Doğan, T., Dehri, İ., 2014. Experimental Studies of 2-Pyridinecarbonitrile as Corrosion Inhibitor for Mild Steel in Hydrochloric Acid Solution. Corrosion Science 82, 125-132.